

# Reaction pathway studies of C<sub>6</sub> hydrocarbons on palladium model catalysts: effects of hydrogen/hydrocarbon ratio, molecular structure, surface structure and temperature

André L.D. Ramos<sup>a,b</sup>, Seong Han Kim<sup>a</sup>, Peilin Chen<sup>a</sup>, Jae Hee Song<sup>a</sup> and Gabor A. Somorjai<sup>a,\*</sup>

<sup>a</sup> Department of Chemistry, University of California, Berkeley, CA 94720-1460, USA and Materials Sciences Division, Lawrence Berkeley National Laboratory, University of California, Berkeley, CA 94720, USA  
E-mail: somorjai@socrates.berkeley.edu

<sup>b</sup> NUCAT-COPPE/EQ, Universidade Federal do Rio de Janeiro, Caixa Postal 68502, CEP 21941, Rio de Janeiro, RJ, Brazil

Received 12 January 2000; accepted 15 March 2000

Reaction pathways of C<sub>6</sub> hydrocarbons, such as hydrogenolysis, dehydrogenation, aromatization and dehydrocyclization, have been studied on small surface area palladium model catalysts, including Pd(111) single crystal and polycrystalline palladium foil. These reactions were performed in a batch reactor, at atmospheric pressure and at two different temperatures (573 and 673 K).

**Keywords:** hexane, palladium model catalysts, Pd(111), hydrogenolysis, hydrocracking, hydrogen, hydrocarbons

## 1. Introduction

Catalytic conversion of alkanes has been studied extensively in the last decades. The main motivation is the conversion of conventional petroleum light naphtha feeds (C<sub>6</sub> and C<sub>7</sub> hydrocarbons) into branched aliphatic hydrocarbons and aromatics, which can increase the octane number in the motor gasoline. For this purpose, isomerization and aromatization are the desired reaction pathways, while hydrogenolysis and dehydrogenation are considered as side reactions. However, there is an increasing demand for new routes to convert conventional feeds into valuable olefins (such as ethylene and propylene) through the use of catalysts, as an alternative for steam cracking. Catalytic hydrogenolysis of C<sub>6</sub> hydrocarbons on palladium would be a promising candidate, since palladium is known to have higher selectivity toward hydrogenolysis.

Zeolites and platinum catalysts have unique selectivity for isomerization and aromatization reaction pathways. For this reason, they are the most studied systems in the literature. The mechanisms of hydrocarbons reforming reactions on platinum have been studied in great detail and have been reviewed by several authors [1–3]. Compared to platinum, fewer studies have been done on palladium for these types of reactions. Some experiments were performed on films [4–6], powders [7,8], palladium black [9,10] and supported catalysts [11–21]. The reforming reaction mechanisms on palladium and other metals were reviewed by Gault [3]. In general, palladium has shown higher selectivity toward hydrogenolysis and dehydrogenation than platinum. Up to date, it is known that a single demethylation (production of C<sub>1</sub> and C<sub>5</sub> hydrocarbons in the same amount) on the

less-substituted carbons is favored on palladium catalysts [3,8–14,17].

In this study, we have employed Pd(111) single crystals and polycrystalline Pd foils as model catalysts and various C<sub>6</sub> hydrocarbons as model reactants. The use of an ultrahigh vacuum (UHV) system equipped with an internal high-pressure reaction cell ensures a well-characterized surface and guarantees minimum contamination. The absence of support eliminates possible metal–support interactions, therefore, only the intrinsic catalytic behavior of palladium is analyzed at lower conversion (<2%). We have found several major differences compared to the studies of palladium supported catalysts, such as the occurrence of internal bond breakage in the hydrogenolysis reaction, high dehydrogenation selectivity and the absence of isomerization on our model systems. To understand the mechanism of hydrogenolysis reactions on the palladium model catalysts, we have also studied the effects of hydrogen/hydrocarbon ratio, molecular structure of the hexane isomers and surface structure of palladium in the hydrogenolysis product distribution.

## 2. Experimental

All of the experiments were carried out in an ultrahigh-vacuum (base pressure =  $5 \times 10^{-10}$  Torr) high-pressure (1 atm) chamber, described previously [22], which was designed to combine surface analysis and catalytic studies using small-area catalyst samples. The chamber is equipped with a retarding field analyzer (RFA) for Auger electron spectroscopy (AES), an argon ion gun for crystal cleaning and a Balzers QMG 421C quadrupole mass spectrometer for residual gas analysis.

\* To whom correspondence should be addressed.

The palladium polycrystalline foil used in this study was 0.125 mm thick, with a surface area of about 1 cm<sup>2</sup> and a purity of 99.99+ % (Goodfellow). The Pd(111) single crystal sample was about 0.7 mm thick, with a surface area of 1 cm<sup>2</sup> and was cut with 0.5° precision. Both sides of crystal were polished using standard techniques.

Samples were cleaned by cycles of Ar<sup>+</sup> bombardment ( $P_{\text{Ar}} = 2 \times 10^{-5}$  Torr,  $T = 773$  K), oxygen treatment ( $P_{\text{O}_2} = 2 \times 10^{-5}$  Torr,  $T = 823$  K) and annealing in UHV at 923 K. The surface cleanliness was then checked by AES. After the cleaning procedure, the sample was enclosed in the high-pressure cell and pressurized at 1 atm. Reactions were carried out in a batch mode in a reaction loop volume of 249 cm<sup>3</sup> and recirculated at flow rate of about 340 cm<sup>3</sup> min<sup>-1</sup>. Normal-hexane (nHx) (Fluka, 99.7%), 2-methylpentane (2MP) (Fluka, 99+%), 3-methylpentane (3MP) (Fluka, 99+%), cyclohexane (cHx) (Fluka, 99+%) and hydrogen (Airgas, ultrahigh purity) were the reactants used in this work. The hydrocarbons (HC) were freeze-pump-thaw degassed three times before experiments. The reaction rates were measured at two different temperatures (573 and 673 K), with a constant hydrocarbon partial pressure (1.6 Torr) and hydrogen pressure ranging from 0 to 128 Torr. Argon was used to make up pressure to 760 Torr. During the reaction, the products were analyzed using an on-line gas chromatograph (Hewlett-Packard 5890) equipped with a flame ionization detector and a GS-alumina, 30 m × 0.53 mm I.D. PLOT column (J&W). The overall conversion was kept lower than 2% to avoid secondary reaction. One important aspect of this work was to avoid the formation of palladium hydride. Therefore, the sample was kept at 383 K during the introduction of reactants and the high-pressure cell was evacuated after reaction at 373 K. Under these conditions, the palladium-hydrogen phase diagram is far from the  $\beta$ -PdH<sub>x</sub> phase [23], and only soluble bulk hydrogen was present, which did not damage the structure of the crystal.

### 3. Results

Reaction products in the *n*-hexane reaction were divided into four reaction pathways as denoted: (a) hydrogenolysis producing C<sub>1</sub> (methane), C<sub>2</sub> (ethane and ethylene), C<sub>3</sub> (propane and propylene), C<sub>4</sub> (butanes and butenes) and C<sub>5</sub> (pentanes and penteres); (b) dehydrocyclization producing cycloalkanes and cycloalkenes; (c) dehydrogenation producing hexenes; (d) aromatization producing benzene. No isomerization products such as methylpentanes were detected under these reaction conditions.

Figure 1(a) shows the accumulated hydrogenolysis production for palladium foil at 573 K as a function of H<sub>2</sub>/nHx ratio. The product distributions for H<sub>2</sub>/nHx ratio larger than 30 at the same temperature are depicted in figure 1(b). Both plots were based on the accumulated production in the batch reactor for 86 min. Alkanes were produced selectively over alkenes (not shown in the plot). At the absence of hydrogen, hydrogenolysis did not occur. At H<sub>2</sub>/nHx = 10,

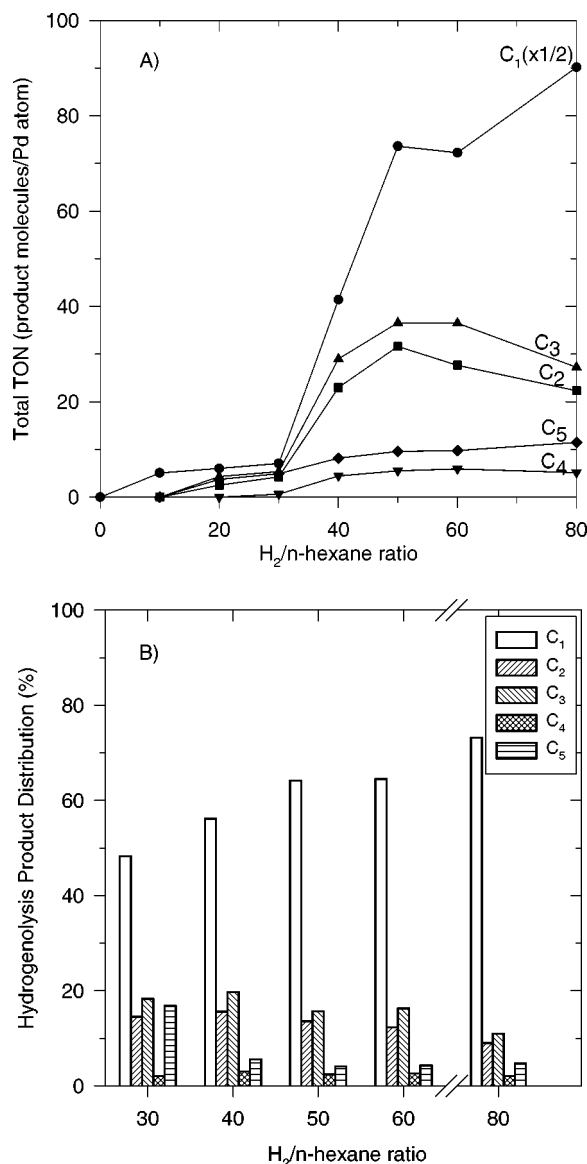


Figure 1. (A) Hydrogenolysis productions and (B) product distributions ( $H_2/nHx \geq 30$ ) in the reaction of *n*-hexane over Pd foil at 573 K as a function of  $H_2/nHx$  ratio based on the accumulated production at  $t = 86$  min. Conditions:  $P_{nHx} = 1.6$  Torr and  $P_{total} = 760$  Torr.

methane was the only hydrogenolysis product. The hydrogenolysis activity remained low until  $H_2/nHx = 30$ . When this ratio reached 40, all the hydrogenolysis products increased considerably. For  $H_2/nHx > 30$ , there was a general production trend following the order:  $C_1 \gg C_3 > C_2 > C_5 > C_4$ . Methane production always increased as the  $H_2/nHx$  ratio increased. Other products did not change substantially at higher  $H_2/nHx$  ratios. The selectivity for C<sub>2</sub> and C<sub>3</sub> was maximum at  $H_2/nHx$  ratio near 40.

At 673 K, hydrogenolysis showed similar behavior with different production trend:  $C_1 \gg C_2 > C_3 > C_4 > C_5$ . For the product distribution, methane production was more dominant at 673 K than at 573 K. However, the overall product distribution did not show strong  $H_2/nHx$  ratio dependence compared to the distribution at 573 K.

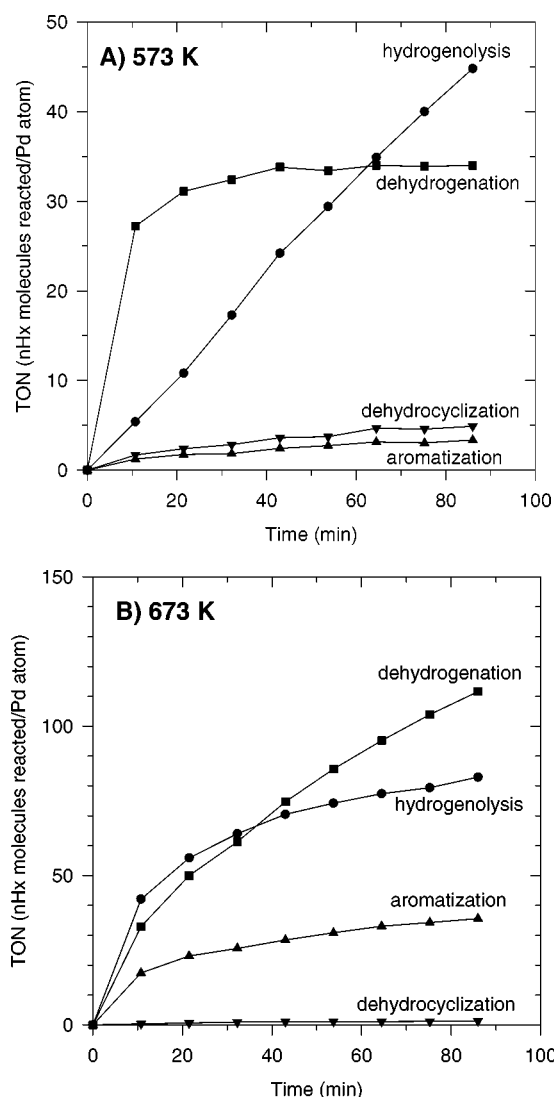


Figure 2. Accumulation plot (number of turnovers versus time) in the reaction of *n*-hexane over Pd foil at (A) 573 and (B) 673 K; conditions:  $P_{H_2} = 64$  Torr,  $P_{nHx} = 1.6$  Torr,  $P_{Ar} = 694$  Torr; (●) hydrogenolysis, (■) dehydrogenation, (▲) aromatization and (▼) dehydrocyclization.

Figure 2 (a) and (b) shows a typical accumulation plot for all the reaction pathways at  $H_2/nHx = 40$ . At 573 K, hydrogenolysis production increased linearly without significant deactivation, while dehydrogenation production leveled off very fast (within 30 min). Aromatization and dehydrocyclization productions were very small at this temperature. At 673 K, hydrogenolysis deactivation was faster, and the yields of dehydrogenation and aromatization were much higher and did not level off. These trends were observed at all  $H_2/nHx$  ratios used in this study as well as a similar dehydrogenation product distribution (*t*-2-hexene > *cis*-2-hexene  $\approx$  *t*-3-hexene > 1-hexene  $\approx$  *c*-3-hexene).

In order to study the effect of reactant structure, reactions of series of C<sub>6</sub> hydrocarbons (HC) were performed on Pd foil under the same conditions.  $H_2/HC$  ratio of 40 was chosen in order to favor the hydrogenolysis reaction pathway but to avoid a higher methane yield. Hydrocarbons used in

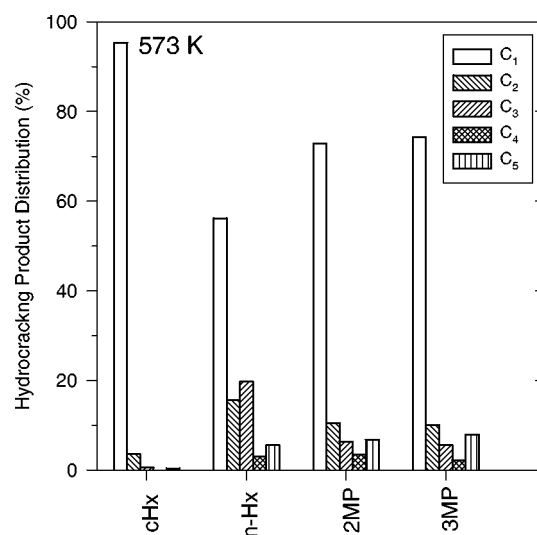


Figure 3. Surface structure effect in the *n*-hexane hydrogenolysis products at 573 and 673 K; conditions:  $P_{H_2} = 64$  Torr,  $P_{nHx} = 1.6$  Torr and  $P_{Ar} = 694$  Torr.

this study were *n*-hexane (nHx), 2-methylpentane (2MP), 3-methylpentane (3MP) and cyclohexane (cHx). The definition of the reaction pathways was the same as the one presented for the *n*-hexane reaction.

2MP, 3MP and nHx had similar activities (same order of magnitude) for all the reaction pathways at both temperatures. Cyclohexane had similar hydrogenolysis activity, but much higher aromatization activity (50 times higher than hydrogenolysis). The production distributions presented in this paper are under similar conversion conditions (0.5% at 573 K, 1% at 673 K). The hydrogenolysis product distributions for all the C<sub>6</sub> hydrocarbons at 573 K are depicted in figure 3. Among these hydrocarbons, cHx had a unique behavior that was a high selectivity toward methane (~95%) at 573 and 673 K. Its distribution pattern did not change appreciably at different temperature. For the non-cyclic hydrocarbons, nHx had the following production distribution:  $C_1 \gg C_3 > C_2 > C_5 > C_4$  at 573 K while branched alkanes (2MP, 3MP) followed the trend:  $C_1 \gg C_2 \approx C_5 > C_3 > C_4$ . Methane yield was higher for branched alkanes, whereas C<sub>2</sub> and C<sub>3</sub> yields were higher in nHx. At 673 K, all the non-cyclic alkanes had very similar product distribution:  $C_1 \gg C_2 > C_3 > C_4 > C_5$ .

The surface structure effect was investigated by comparing the reactivity of Pd(111) and palladium foil. Initial turnover frequencies for Pd(111) single crystal and palladium polycrystalline foil are listed in table 1. Reactions were performed under the same conditions for both samples. Pd foil always showed higher reactivity than Pd(111) for all the reactions. For the hydrogenolysis reaction, Pd foil showed much stronger temperature dependence. The difference in reactivity between both catalysts has increased from 1.6 fold at 573 K to 6.7 fold at 673 K.

Table 2 shows the reaction selectivity comparison at the end of reaction ( $t = 86$  min). Pd foil showed higher selectivity toward hydrogenolysis, while Pd(111) was more

Table 1  
Activity surface structure comparison in the reaction of *n*-hexane over Pd model catalysts.<sup>a</sup>

Reaction	Initial turnover frequency (nHx molecules reacted (Pd atom) <sup>-1</sup> s <sup>-1</sup> ) <sup>b</sup>					
	<i>T</i> = 573 K			<i>T</i> = 673 K		
	Pd foil	Pd(111)	Pd foil/Pd(111)	Pd foil	Pd(111)	Pd foil/Pd(111)
Hydrocracking	0.0085	0.0052	1.6	0.0652	0.0098	6.7
Dehydrogenation	0.0421	0.0382	1.1	0.0510	0.0363	1.4
Aromatization	0.0019	0.0008	2.4	0.0269	0.0132	2.0

<sup>a</sup> Conditions:  $P_{\text{nHx}} = 1.6$  Torr,  $P_{\text{H}_2} = 64$  Torr and  $P_{\text{Ar}} = 694$  Torr.

<sup>b</sup> The error bars were about 10% for Pd foil and 25% for Pd(111).

Table 2  
Selectivity surface structure comparison in the reaction of *n*-hexane over Pd model catalysts.<sup>a</sup>

Reaction	Reaction selectivity <sup>b</sup> (%)			
	<i>T</i> = 573 K		<i>T</i> = 673 K	
	Pd foil	Pd(111)	Pd foil	Pd(111)
Hydrocracking	52	27	36	19
Dehydrogenation	39	64	48	58
Dehydrocyclization	5	4	1	1
Aromatization	4	5	15	22

<sup>a</sup> Conditions:  $P_{\text{nHx}} = 1.6$  Torr,  $P_{\text{H}_2} = 64$  Torr and  $P_{\text{Ar}} = 694$  Torr.

<sup>b</sup> Based on the accumulated products at  $t = 86$  min. Reaction selectivity is defined as the carbon percentage of nHx consumed in the formation of a designated product.

selective to dehydrogenation. Aromatization and dehydrocyclization selectivities were almost the same for both catalysts. These trends were observed at both temperatures.

#### 4. Discussion

Several bond-breaking mechanisms may contribute to the hydrogenolysis product distribution. The main competition is between single and multiple bond breakage of the hydrocarbon molecule. Multiple bond breakage is the consecutive breakage of the hydrocarbon molecule in several bonds which mainly produces methane. Single bond breakage can be subdivided into terminal and internal bond breakage. Terminal bond breakage yields C<sub>1</sub> and C<sub>5</sub> hydrocarbon molecules (demethylation), while internal bond breakage can be a deethylation (producing C<sub>2</sub> and C<sub>4</sub> molecules) or a depropylation (producing two C<sub>3</sub> molecules).

A good parameter to evaluate the competition between these mechanisms is the fission parameter. The fission parameter ( $M_f$ ) for hydrogenolysis reactions of hydrocarbons containing  $n$  carbon atoms is defined [24] as

$$M_f = [C_1]^{-1} \sum_{i=2}^n \sum_j (n-i)[C_i]j, \quad (1)$$

where the summation over  $j$  includes all products with  $i$  carbon atoms. For C<sub>6</sub> hydrocarbons hydrogenolysis ( $n = 6$ ),  $M_f$  can be expressed as

$$M_f = (4C_2 + 3C_3 + 2C_4 + C_5)/C_1. \quad (2)$$

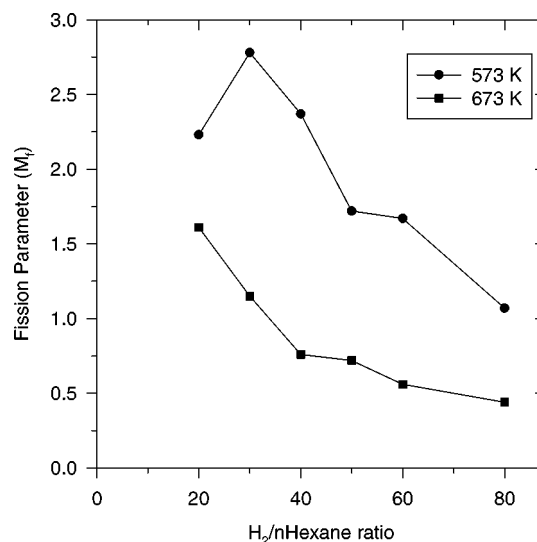


Figure 4. Fission parameters as a function of H<sub>2</sub>/nHx ratio in the reaction of *n*-hexane on Pd foil. Conditions:  $P_{\text{nHx}} = 1.6$  Torr and  $P_{\text{total}} = 760$  Torr.

For  $M_f$  higher than one, the internal single bond breakage is the dominant mechanism which yields mainly C<sub>2</sub> and C<sub>3</sub> hydrocarbons.  $M_f$  close to one indicates a preference for terminal single bond breakage, yielding C<sub>1</sub> and C<sub>5</sub> hydrocarbons in the same amount.  $M_f$  lower than one means a preference for sequential multiple bond breakage, yielding methane.

Figure 4 shows the fission parameter as a function of H<sub>2</sub>/n-hexane ratio. This analysis, together with the product distribution presented in figure 1, allows us to identify the dominant hydrogenolysis mechanism and the influence of the H<sub>2</sub>/nHx ratio.

At 573 K, no hydrogenolysis production was detected at low H<sub>2</sub>/nHx ratios (H<sub>2</sub>/nHx = 0, 10), therefore, no fission parameters were calculated at these ratios. At medium H<sub>2</sub>/nHx ratios (H<sub>2</sub>/nHx = 20, 30, 40), higher fission parameters were observed, indicating a preference for single bond breakage. Since C<sub>3</sub> production was always higher than C<sub>5</sub>, internal bond breakage was the preferred channel. Deethylation (production of C<sub>2</sub> and C<sub>4</sub> hydrocarbon units) was not favored, because C<sub>2</sub> production was much higher than C<sub>4</sub> independent of the H<sub>2</sub>/nHx ratio, which was in agreement with the literature data [3]. Most of the ethane might be the result of multiple bond breakage. At higher H<sub>2</sub>/nHx ratios (H<sub>2</sub>/nHx = 80), multiple bond breakage be-



came important, which can be seen by the increase of C<sub>1</sub> production at the expense of C<sub>2</sub> and C<sub>3</sub> production, and the decrease of fission parameters. However, single bond breakage was still the main mechanism, because the fission parameter was always higher than one. The fact that the production of C<sub>2</sub> through C<sub>5</sub> hydrocarbons did not change substantially for H<sub>2</sub>/nHx > 30 may imply that the single bond breakage rate did not depend on the hydrogen pressures, while multiple bond breakage rate still increased with this ratio. The preference for internal bond breakage was a surprising result, as it has always been associated to platinum catalysts [3]. This type of behavior has never been observed in palladium supported catalysts.

At 673 K, the product distribution did not change substantially with H<sub>2</sub>/nHx ratio. Fission parameter decreased monotonically with H<sub>2</sub>/nHx ratio, showing an increase in multiple bond breakage. At H<sub>2</sub>/nHx ≥ 40, fission parameters were lower than one indicating that multiple bond breakage started to dominate. The other observation was the general production trend at this temperature: C<sub>1</sub> ≫ C<sub>2</sub> > C<sub>3</sub> > C<sub>4</sub> > C<sub>5</sub>, which follows a Schulz–Flory distribution. This distribution suggests the formation of C<sub>1</sub> units on Pd surface and further formation of the other hydrocarbons by coupling reactions.

Concerning the reaction pathways, the catalytic results presented in this study show considerable differences compared to those reported in the literature for palladium supported catalysts. First of all, the dehydrogenation selectivity was generally higher, which can be seen in table 2. Most of the authors have reported a very low (<1%) rate of dehydrogenation in the reaction of C<sub>6</sub> non-cyclic hydrocarbons on palladium supported catalysts [11,16–20]. Paál and Tétényi have reported dehydrogenation selectivity of about 15% in the reaction of methylpentanes over Pd powders [10], and Ivanova et al. have found the dehydrogenation selectivity decreased drastically with conversion in the reaction of Pd/Mg(Al)O in a flow system [13]. Several authors, using metal supported and zeolite catalysts, have proposed that hexenes would be unstable with respect to self-hydrogenation [25,26], aromatization [27,28] and coke formation [29,30]. The low conversions employed in the present study would minimize the occurrence of these side reactions, allowing the high selectivity toward dehydrogenation in most of the reactions.

Another result that needs to be pointed out is the absence of isomerization production. So far, palladium was considered to exhibit some, generally low, activity for isomerization products. Contreras et al. have observed isomerization selectivity of 57% in the reaction of *n*-hexane over Pd/Al<sub>2</sub>O<sub>3</sub> at 523 K [11]. Juszczak et al. have shown isomerization selectivity ranges of 23–50% (Pd/SiO<sub>2</sub>) and 13–96% (Pd/Al<sub>2</sub>O<sub>3</sub>) in the reaction of nHx [20,21]. Normand et al. have reported an isomerization selectivity range of 41–71% in the reaction of 2-methylpentane at 573 K on Pd/Al<sub>2</sub>O<sub>3</sub> catalysts [17]. The main reason for the absence of isomerization production in our model catalysts should be related to the absence of certain sites, which were claimed to favor

Table 3  
Fission parameters in the hydrocracking of hexane isomers.<sup>a</sup>

Hydrocarbon	$M_f$	
	573 K	673 K
nHx	2.37	0.76
2MP	1.03	0.61
3MP	0.93	0.66

<sup>a</sup> Based on the accumulated products at  $t = 86$  min. Conditions:  $P_{\text{nHx}} = 1.6$  Torr,  $P_{\text{H}_2} = 64$  Torr and  $P_{\text{Ar}} = 694$  Torr.

isomerization selectivity in other systems, such as acidic sites [20,21] and sites resulting from the use of bimetallic materials [31] and metal–support interactions [16,20,21].

For the time-dependent behavior in the product distribution, the production accumulation was different at 573 and 673 K, as can be seen in figure 2. At 573 K, dehydrogenation production ceased within 30 min while it did not level off at 673 K. Coke formation can be ruled out, since this fast cease of production was not seen at higher temperature (673 K), which would favor its formation. A possible explanation might be different hydrogen coverages at both temperatures. From isotope exchange studies, it was clear that the first step in the hydrocarbon conversion reactions was the dissociation of one C–H bond [32]. This occurred at much lower temperature than any other possible reaction. The further reactions over a given metal would be governed in a great extent by the amount of hydrogen available. Dehydrogenation is a reversible reaction under these conditions, and hydrogen is a reaction product. At lower temperature (573 K), hydrogen coverage is higher, which would shift the equilibrium toward alkane formation. The considerable increase in aromatization production with temperature might be explained by the same reason, since this reaction is also reversible, endothermic and hydrogen is a reaction product, in such a way that a lower hydrogen coverage at higher temperature would favor aromatization production.

The different behavior of cyclohexane hydrogenolysis compared to the non-cyclic C<sub>6</sub> alkanes implies that they proceed via a different mechanism on the palladium surface. Cyclohexane hydrogenolysis had a much higher methane yield, and its product distributions did not change with temperature whereas the hydrogenolysis of non-cyclic C<sub>6</sub> alkanes had a lower methane yield and depended on the temperature. It is well accepted in the literature that hydrogenolysis reaction of non-cyclic alkanes occurs by a bond-shift isomerization mechanism, instead of a cyclic mechanism [3]. The results obtained in this work confirm this assumption.

For non-cyclic alkanes, there is a strong effect of the reaction temperature, as can be seen in figure 4 and table 3, which present the fission parameters in the hydrogenolysis of the non-C<sub>6</sub> cyclic alkanes. At 573 K, it is clear that internal single bond breakage was favored in the linear hydrocarbon (nHx), giving a higher C<sub>2</sub> and C<sub>3</sub> yield, therefore, a higher fission parameter. Single terminal bond breakage was preferred in the branched isomers, since methane and

C<sub>5</sub> yields were higher in the reaction of these molecules, and the fission parameter was close to one. At 673 K, all the hexane isomers had similar product distribution and fission parameters less than one, implying that multiple bond breakage was the dominant mechanism for all the molecules under these conditions, without a molecular structure sensitivity.

Tables 1 and 2 show that there are some differences in the catalytic results with the surface structure. Pd(111) was more selective to dehydrogenation and less selective to hydrogenolysis at both temperatures. At 573 K, in the hydrogenolysis product distribution there was a small trend of higher selectivity toward C<sub>1</sub> hydrocarbon at the expense of C<sub>2</sub> and C<sub>3</sub> production on Pd(111). It can be clearly seen by the fission parameter which was about 2.37 on Pd foil and 1.45 on Pd(111), suggesting a lower internal bond breakage rate on the later surface. At 673 K, fission parameters on Pd foil and Pd(111) were 0.76 and 0.79, respectively. Both product distribution and fission parameters were very similar on both surfaces, indicating a similar hydrogenolysis mechanism.

One point that should be highlighted is the difference in increasing of hydrogenolysis activity with temperature. The fact that Pd foil had an eight-fold increase, while Pd(111) had a two-fold increase when the temperature was raised from 573 to 673 K suggests a structure sensitivity at higher temperatures. Reactions of several alkanes on platinum model catalysts [33] have shown that the hydrogenolysis of *n*-butane and *n*-hexane had little dependence on platinum surface structure at 573 K. However, stepped and kinked platinum surfaces with (111) terraces, which are the major sites on polycrystalline foil, were several times more active than the flat low-index crystal faces for isobutane and neopentane hydrogenolysis. We have also found a low structure sensitivity in the *n*-hexane reaction at 573 K, however, polycrystalline Pd foil (which has stepped and kinked surfaces) exhibited about seven times more active for hydrogenolysis at 673 K, which suggested that the structure sensitivity occurred only at higher temperatures, but with a similar bond breaking mechanism, since the product distribution and fission parameters were almost the same for both surfaces.

## 5. Conclusions

Reforming reaction pathways of C<sub>6</sub> hydrocarbons have been studied on small surface area palladium model catalysts using various H<sub>2</sub>/hydrocarbon ratios at two temperatures. Methane was found to be the predominant product as the result of hydrogenolysis. Hydrogenolysis and dehydrogenation were the key reaction pathways in these reactions and aromatization was only important at higher temperature. At higher temperature, the structure sensitivity was also observed.

For the hydrogenolysis of C<sub>6</sub> alkanes at 573 K, there were three types of bond breaking mechanisms: single terminal bond breakage was significant at low H<sub>2</sub>/hydrocarbon

ratios and for the branched alkanes. Single internal bond breakage was generally favored, especially in the reaction of *n*-hexane at medium H<sub>2</sub>/hydrocarbon ratios. Multiple bond breakage was meaningful at higher H<sub>2</sub>/hydrocarbon ratios. At 673 K, multiple bond breakage was dominant independent of the reactant molecules, H<sub>2</sub>/hydrocarbon ratios and surface structure. Cyclohexane hydrogenolysis had a completely different behavior compared to the non-cyclic C<sub>6</sub> alkanes, implying that the hydrogenolysis of cyclic and non-cyclic alkanes proceed via a different mechanism on palladium surface.

Dehydrogenation selectivity was significant at lower hydrogen/hydrocarbon ratios, which was ascribed to the low conversions employed in this study. Dehydrogenation reaction leveled off at 573 K, which was not observed at 673 K, was probably due to a lower hydrogen coverage. Isomerization products could not be detected under the reaction conditions used in the study, which was attributed to the absence of acidic sites and metal-support interactions.

Pd(111) single crystal was more selective to dehydrogenation and had a higher selectivity toward C<sub>1</sub> hydrocarbon at the expense of C<sub>2</sub> and C<sub>3</sub> production at 573 K, suggesting that internal bond breakage was less important on this surface. Surface structure sensitivity was observed at higher temperature (673 K), whereas Pd foil was about seven times more active for hydrogenolysis than Pd(111) single crystal.

## Acknowledgement

This work has been supported by Office of Energy Research and Office of Basic Energy Sciences of the US Department of Energy and a fellowship from CNPq-Brazil.

## References

- [1] J.R. Anderson, *Adv. Catal.* 23 (1973) 1.
- [2] J.K.A. Clarke and J.J. Rooney, *Adv. Catal.* 25 (1976) 125.
- [3] F.G. Gault, *Adv. Catal.* 30 (1981) 1.
- [4] J.R. Anderson and N.R. Avery, *J. Catal.* 5 (1966) 446.
- [5] J.R. Anderson and N.R. Avery, *J. Catal.* 2 (1963) 542.
- [6] J.K.A. Clarke and J.F. Taylor, *J. Chem. Soc. Faraday Trans.* 72 (1976) 917.
- [7] J.L. Carter, J.A. Cusumano and J.H. Sinfelt, *J. Catal.* 20 (1971) 223.
- [8] M. Hajek, S. Corolleur, C. Corolleur, G. Maire, A. O'Cinneide and F.G. Gault, *J. Chim. Phys.* 71 (1974) 1329.
- [9] Z. Paál and P. Tétényi, *React. Kinet. Catal. Lett.* 12 (1979) 131.
- [10] Z. Paál and P. Tétényi, *Appl. Catal.* 1 (1981) 9.
- [11] J.L. Contreras, J.M. Ferreira, S. Fuentes and R. Gómez, *React. Kinet. Catal. Lett.* 7 (1977) 373.
- [12] I.I. Ivanova, M. Seirvert, A. Pasau-Claerbout, N. Blom and E.G. Derouane, *J. Catal.* 164 (1996) 347.
- [13] I.I. Ivanova, A. Pasau-Claerbout, M. Seirvert, N. Blom and E.G. Derouane, *J. Catal.* 158 (1996) 521.
- [14] A. O'Cinneide and F.G. Gault, *J. Catal.* 37 (1975) 311.
- [15] W. Juszczuk and Z. Karpinski, *J. Catal.* 117 (1989) 519.
- [16] W. Juszczuk, Z. Karpinski, I. Ratajczykowa, Z. Stanasiuk, J. Zielinski, L.-L. Sheu and W.M.H. Sachtler, *J. Catal.* 120 (1989) 68.
- [17] F. Le Normand, K. Kili and J.L. Schmitt, *J. Catal.* 139 (1993) 234.

- [18] W. Juszczuk, Z. Karpinski, J. Pielaszek and Z. Paál, *J. Catal.* 143 (1993) 583.
- [19] A. Malinowski, W. Juszczuk, D. Lomot, J. Pielaszek and Z. Karpinski, *Polish J. Chem.* 69 (1995) 308.
- [20] D. Lomot, W. Juszczuk, J. Pielaszek and Z. Karpinski, *Polish J. Chem.* 69 (1995) 1551.
- [21] D. Lomot, W. Juszczuk and Z. Karpinski, *Appl. Catal. A* 155 (1997) 99.
- [22] D.W. Blakely, E. Kosak, B.A. Sexton and G.A. Somorjai, *J. Vac. Sci. Technol.* 13 (1976) 1901.
- [23] F.H. Ribeiro, C.A. Gerken, G.A. Somorjai, C.S. Kellner, G.W. Coulston, L.E. Manzer and L. Abrams, *Catal. Lett.* 45 (1997) 149.
- [24] V. Ponec and W.M.H. Sachtler, in: *Proc. 5th Int. Congr. Catal.* (1972) p. 645.
- [25] M. Pruski, J.C. Kelzenberg, B.C. Gerstein and T.S. King, *J. Am. Chem. Soc.* 112 (1990) 4232.
- [26] Y.S. Kye, S.X. Wu and T.M. Apple, *J. Phys. Chem.* 96 (1992) 2632.
- [27] M.J. Lambregts, E.J. Munson, A.A. Kheir and J.F. Haw, *J. Am. Chem. Soc.* 114 (1992) 6875.
- [28] I.I. Ivanova, N. Blom, S.B. Abdul Hamid and E.G. Derouane, *Rec. Trav. Chim. Pays-Bas* 113 (1994) 454.
- [29] J.L. White, N.D. Lazo, B.R. Richardson and J.F. Haw, *J. Catal.* 125 (1990) 260.
- [30] P.K. Wang, C.P. Slichter and J.H. Sinfelt, *J. Phys. Chem.* 89 (1985) 3606.
- [31] C. Visser, J.G.P. Zuidwijk and V. Ponec, *J. Catal.* 35 (1974) 407.
- [32] P. Tétényi, L. Guzzi and A. Sárány, *Acta Chim. Acad. Sci. Hung.* 97 (1978) 221.
- [33] S.M. Davis, F. Zaera and G.A. Somorjai, *J. Am. Chem. Soc.* 104 (1982) 7453.